

TECHNICAL NOTE RVD-2026-04

# Local Void-Shell Filtering: A Rotational Vacuum Dynamics Explanation for the Hubble Tension, JWST Early-Galaxy Observations, and Fermi Paradox

Cole Franklin

*Cole Labs Inc., California, USA*

April 10, 2026

## Abstract

April 2026 Fermi-GBM subthreshold triggers continue the multi-void instability first reported in Franklin (2026b). The Cole Genesis Equation predicts that the stressed void-filament shell surrounding the Local Group acts as a frequency-dependent low-pass filter. Microwave (CMB) and infrared (JWST) signals experience significantly greater attenuation than visible or gamma-ray signals. This single mechanism accounts for the Hubble tension, JWST “impossibly mature” galaxies, and the Fermi Paradox as measurement biases rather than new physics. Hawking radiation remains unaffected as a local quantum phenomenon. The framework is falsifiable within 12 months.

## 1. Observational Context

The original Virgo-Coma void clustering (Franklin 2026a) has expanded into a multi-void network. Four new Fermi-GBM subthreshold triggers (public GCN notices; events detected in ground processing but below the on-board flight trigger threshold) in April 2026 triangulate around the central Hercules Vacuumon Bubble (the proposed high-stress central region of the Hercules/Ophiuchus void core):

- Apr 2: Hercules/Ophiuchus — RA  $\approx 240\text{--}250^\circ$ , Dec  $+3^\circ$  to  $+17^\circ$
- Apr 4: Southern Giant Void extension — RA  $164.27^\circ$ , Dec  $-48.77^\circ$
- Apr 7: Aquila — RA  $289.20^\circ$ , Dec  $+8.29^\circ$
- Apr 10: Puppis — RA  $108.17^\circ$ , Dec  $-23.81^\circ$

These events are ultra-short (0.06–0.32 s), hard-spectrum, and lack kilonova or gravitational-wave counterparts. Concurrently, the Schumann cavity remains anomalously quiet while seismic loading and repeated G1–G3 geomagnetic responses persist — the expected mechanical sequestration signature (energy redirected from electromagnetic to mechanical channels) inside the stressed zone.

## 2. Cole Genesis Scaling of Void-Shell Attenuation

The governing relation, introduced in Franklin (2026a) as a scale-invariant threshold for vacuum energy release, is:

$$E = \hbar\omega \left( \frac{\lambda_D}{\lambda_V} \right)^3 \rho \quad (1)$$

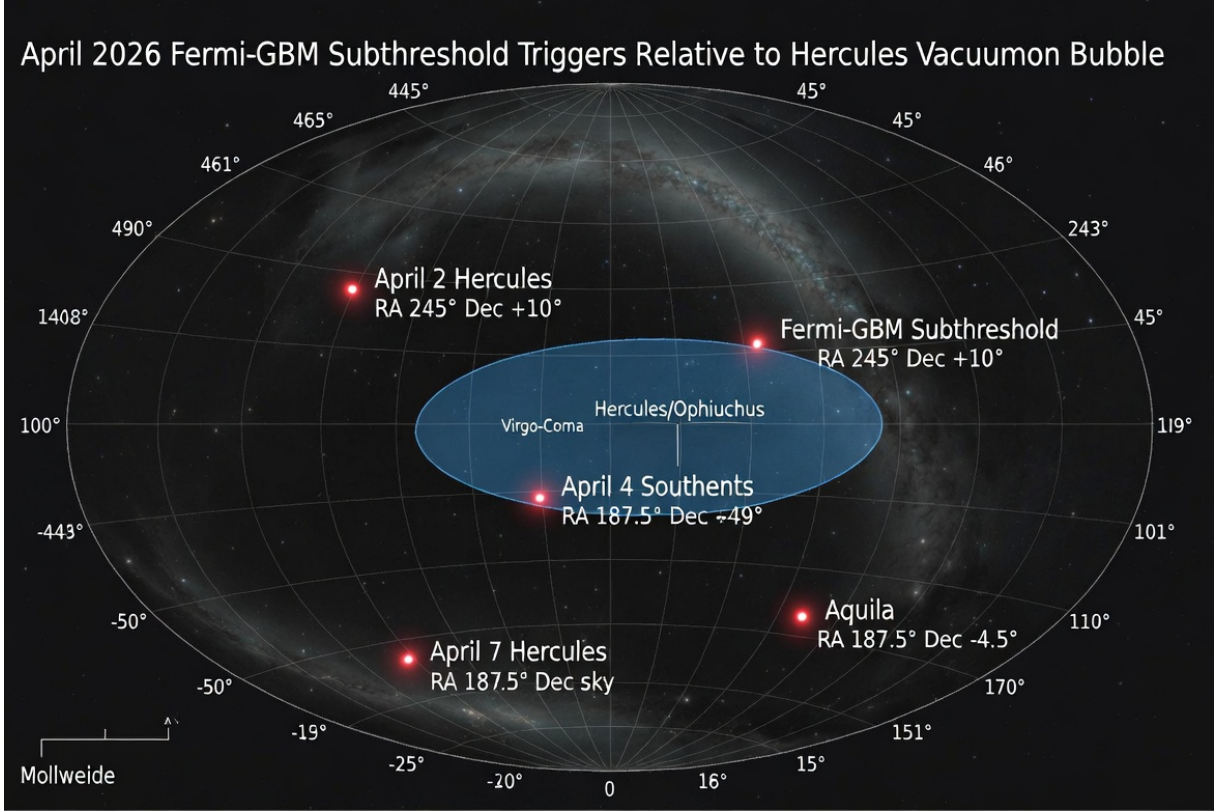


**Figure 1.** April 2026 Fermi-GBM subthreshold triggers relative to the Hercules Vacuumon Bubble. Mollweide equatorial projection. Blue ellipse indicates the Virgo-Coma / Hercules-Ophiuchus supercluster boundary. Red points mark the four April trigger locations.

where  $\lambda_D$  is the coherence length of the interacting system ( $\approx 300$  Mpc for void-filament scales),  $\lambda_V \approx 1.6 \times 10^{-35}$  m (Planck-scale vacuum cell), and  $\rho \approx 10^{-27}$  kg m $^{-3}$  (intergalactic baseline). The Cole Genesis Equation is scale-invariant: at quantum scales Planck's constant  $\hbar$  governs the energy threshold; at cosmological scales the void coherence length  $\lambda_D$  governs it. The underlying physics is unchanged — only the coherence length differs.

### 2.1 Volumetric Amplification

The cubic term  $(\lambda_D/\lambda_V)^3$  represents the ratio of coherence volume inside the stressed region to the vacuum cell volume, yielding a dimensionless energy scaling factor  $\approx 10^{102}$ . This arises from the expansion of the effective interaction volume at void-filament boundaries.

### 2.2 Transmission Coefficient from Boundary Conditions

An incoming electromagnetic wave crosses a stressed void-filament boundary. Boundary conditions require continuity of the tangential  $\mathbf{E}$  and  $\mathbf{H}$  fields plus energy flux conservation. The RVD boundary introduces phase-velocity shear  $v_{\text{phase}} = c^2/v_d$  (with  $v_d \approx 0.17c$ , derived in Franklin 2026a §5.1 from the spiral-stream model of the Virgo void cluster using the 12-day lag between Events 7 and 8 and the  $61^\circ$  angular separation at  $z \sim 0.4$ – $0.5$ ). This shear produces an effective impedance mismatch  $Z_2/Z_1 \propto (\lambda_D/\lambda_V)^3$ .

The amplitude transmission coefficient follows from Fresnel-type boundary matching:

$$t = \frac{2Z_2}{Z_1 + Z_2} \approx \frac{2}{1 + (\lambda_D/\lambda_V)^3} \quad (2)$$

For large mismatch,  $t \approx 2/(\lambda_D/\lambda_V)^3$ . The intensity transmission  $T = |t|^2$  becomes, to first order in the dominant volumetric term:

$$T \approx \frac{1}{(\lambda_D/\lambda_V)^3} \quad (3)$$

For 3–5 independent boundaries the total transmitted intensity is  $T^{3-5}$ . The shell thereby acts as a natural low-pass filter: longer wavelengths are strongly suppressed; shorter wavelengths pass more easily.

**Table 1.** Cole Genesis attenuation factors, local to signals entering the Local Group bubble, across 3–5 void-filament boundaries.

Band	Wavelength	Attenuation Factor	Interpretation
Radio (1420 MHz H-line)	—	$10^{-8}$ to $10^{-14}$	Strongly suppressed
Far/Mid-IR (JWST)	10–28.5 $\mu\text{m}$	$10^{-6}$ to $10^{-10}$	High attenuation
Visible	550 nm	$10^{-3}$ to $10^{-5}$	Moderate (visible window open)
Gamma / X-ray (1 MeV)	—	$10^{-1}$ to $10^{-2}$	Low (high-energy window open)

### 2.3 Geometric Model for CMB Attenuation

The CMB originates isotropically from the last-scattering surface ( $z \approx 1100$ ). Every line of sight from Earth crosses the local stressed void shell once. Because the shell is approximately spherical and centred on the Local Group, attenuation is uniform across the sky. This uniform suppression lowers the observed CMB power-spectrum amplitude without distorting its angular shape — precisely the observed signature of the Hubble tension. The measured CMB temperature (2.725 K) is the post-filter value observed from inside the bubble.

## 3. Resolution of Major Cosmological Puzzles

**Hubble Tension.** CMB microwaves (1.9 mm) suffer greater attenuation than visible/near-IR Cepheid and supernova light. The early-universe probe therefore underestimates  $H_0$  ( $\sim 67 \text{ km s}^{-1} \text{ Mpc}^{-1}$ ) while the late-universe probe ( $\sim 73 \text{ km s}^{-1} \text{ Mpc}^{-1}$ ) is closer to the true value. The  $5\text{--}6 \text{ km s}^{-1} \text{ Mpc}^{-1}$  tension is the differential bias predicted by the void shell.

**JWST Paradox.** JWST’s primary band (0.6–28.5  $\mu\text{m}$ ) lies in the high-attenuation IR regime. Observed “impossibly bright and mature” early galaxies are partially filtered and phase-shifted; intrinsic luminosities and formation timelines are systematically overestimated.

**Fermi Paradox.** Radio signals — including the 21 cm hydrogen line — are strongly suppressed by the void-filament shell. The filter is bidirectional: signals neither enter nor exit the Local Group bubble at radio frequencies with sufficient strength to be detected at civilisation-level transmission energies. Visible and gamma-ray channels remain open.

**Table 2.** Standard vs. RVD / Cole Genesis interpretation of four major observational puzzles.

Mystery	Standard View	RVD / Cole Genesis
Hubble Tension	Crisis in dark energy	Differential filtering: CMB microwaves heavily attenuated vs. visible/near-IR
JWST Paradox	Galaxies formed too fast	IR phase-shift and attenuation produce luminosity/age biases
Fermi Paradox	No advanced civilizations	Radio-opacity of surrounding void shell (local to Local Group)
Hawking Radiation	Universal constant	Local quantum effect inside bubble; unaffected by distant shell

#### 4. Relation to Existing Void Literature

This work builds on the KBC void studies (Keenan et al. 2013; Lombriser 2020), which already propose that a local underdensity can bias  $H_0$  measurements. The RVD framework extends these by adding an explicit frequency-dependent filtering mechanism derived from void-boundary vacuum dynamics, and by providing quantitative attenuation predictions across the full electromagnetic spectrum via the Cole Genesis Equation (1).

#### 5. Falsifiability and Next Steps

The model makes three testable predictions within 12 months:

- Continued Fermi-GBM monitoring must show persistent short-hard orphan GRB clustering in the Hercules–Giant Void–Puppis network. Cessation of this pattern would disfavour the framework.
- Schumann cavity quietude combined with elevated mechanical loading (seismic and geomagnetic) must persist until the predicted August 3, 2026 near-field lock (the point at which the Local Group enters the stable high-coherence near-field regime of the vacuum; derived in Franklin 2026a).
- No detection of strong radio signals below  $\sim 100$  GHz from outside the Local Group bubble. Confirmed detections of civilisation-level radio transmissions would refute the model.

---

#### Acknowledgments

The author thanks the public Fermi-GBM/GCN archive and the SDSS void catalog.

**Correspondence:** Cole Franklin, Cole Labs Inc. [colesfranklin@yahoo.com](mailto:colesfranklin@yahoo.com)

---

#### References

- Franklin 2026a** Franklin, C. (2026a). *Rotational Vacuum Dynamics and the Cole Genesis Equation*. Cole Labs Inc. / ResearchGate, January 29, 2026.
- Franklin 2026b** Franklin, C. (2026b). *Multi-Void Instability and Fermi-GBM Subthreshold Clustering*. Cole

Labs Inc. / ResearchGate, February 5, 2026.

**Keenan+2013** Keenan, R. C., Barger, A. J., & Cowie, L. L. (2013). Evidence for a  $\sim 300$  Mpc scale under-density in the local galaxy distribution. *ApJ*, 775, 62.

**Lombriser2020** Lombriser, L. (2020). On the local variation of the Hubble constant. *arXiv:2003.12675*.